Tetrahedron 195 (2026) 135195

Contents lists available at ScienceDirect

Tetrahedron

journal homepage: www.elsevier.com/locate/tet

Catalyst-free visible-light mediated α-alkylation of quinazolines and pyrrolo[2,1-*f*][1,2,4]triazine

Jhonathan R.N. dos Santos [a], Victor Biagio A. Sciota [a], Geovana F. Vargas [b], Camila Batista Pinto [c], Giovanni W. Amarante [b], Javier Ellena [c], Arlene G. Corrêa [a,*]

[a] Centre of Excellence for Research in Sustainable Chemistry, Federal University of São Carlos, 13565-905, São Carlos, SP, Brazil
[b] Department of Chemistry, Federal University of Juiz de Fora, Juiz de Fora, MG, 36036-900, Brazil
[c] São Carlos Institute of Physics, University of São Paulo, São Carlos, SP, 13563-120, Brazil

ARTICLE INFO

Keywords:
Quinazoline
pyrrolo[2,1-*f*][1,2,4]triazine
Photochemistry
C–H functionalization
N-heterocycles

ABSTRACT

Quinazolines are found in numerous commercially available drugs. Herein, we report a catalyst-free photochemical approach for the direct alkylation of these *N*-heterocycles under mild conditions. Additionally, late-stage functionalization of bioactive natural products—including caffeine, quinine derivative and flavone—was successfully achieved. Notably, the protocol also enabled the selective C7-functionalization of the pyrrolo[2,1-*f*][1,2,4]triazine core without requiring pre-functionalization, representing the first example of this transformation accomplished through a photochemical process. Using the optimized reaction condition, 17 alkylated heterocycles were prepared in 10-81% yield.

1. Introduction

Nitrogen-containing heterocyclic compounds appear in approximately 82% of all drugs approved in the past decade [1]. Among the *N*-heterocycles, quinazolines—particularly 4-aminoquinazolines—are key structural motifs featured in several commercially available pharmaceuticals, such as terazosin and ziresovir [2] (Fig. 1). Likewise, the pyrrolo[2,1-*f*][1,2,4]triazine is an important scaffold, found in kinase inhibitors and nucleoside-based drugs including avapritinib and remdesivir [3]. Given the pharmacological relevance of these *N*-heterocycles, numerous methods have been developed for the synthesis of quinazolines [4] and pyrrolotriazines [5].

The functional groups introduced onto a *N*-heterocyclic core critically influence its physicochemical and biological properties. Therefore, appropriate functionalization of quinazolines and pyrrolotriazines is essential to unlock their broad utility as therapeutic agents and building blocks for new drug candidates [6]. To meet this demand, simple, practical, sustainable, and high-yielding synthetic methods are required for the efficient modification of these *N*-heterocycles. In recent years, late-stage C–H functionalization has emerged as a remarkably versatile strategy. Such transformations can be promoted electrochemically [7] or photochemically [8], and may proceed with or without transition-metal catalysts.

Although C–H activation of quinazolinones have been explored [9], few examples using quinazolines are described [10]. Concerning the pyrrolotriazine, its functionalization is typically achieved through the corresponding halide derivatives, often requiring harsh conditions [11]. Notably, List and co-workers reported a silylium-catalyzed C-glycosylation of pyrrolo[2,1-*f*][1,2,4]triazine that proceeds without the need for pre-installed protecting or activating groups [12].

In this context, photochemistry has emerged as a powerful strategy for the direct C–H functionalization of heterocycles, notably through Minisci-type reactions. These transformations proceed via radical nucleophilic substitution ($S_{RN}1$) mechanisms, in which radical species can be generated through decarboxylation, hydrogen atom transfer (HAT), electrochemical methods, or photochemical activation of Katritzky salts, dihydropyridines (DHPs) and other radical precursors [13]. The Gutierrez-Bonet group [14] reported the use of DHPs in the presence of an oxidant to enable the direct functionalization of quinazolin-4-ones. Similarly, Chen et al. demonstrated the visible-light-mediated, chemoselective C–H functionalization of peptides using 4-alkyl-DHPs [15]. Peptide functionalization has also been achieved under photoredox conditions employing carbamoyl-DHPs as radical precursors [16].

This article is part of a special issue entitled: Brazil published in Tetrahedron.

* Corresponding author.
E-mail address: agcorrea@ufscar.br (A.G. Corrêa).

https://doi.org/10.1016/j.tet.2026.135195
Received 12 December 2025; Received in revised form 9 February 2026; Accepted 16 February 2026
Available online 18 February 2026

Therefore, continuing our efforts to develop greener methods for the functionalization of *N*-heterocycles [17], we report herein the first photochemical approach for the direct alkylation of aminoquinazolines and pyrrolo[2,1-*f*][1,2,4]triazine under mild conditions.

2. Results and discussion

Based on the work developed by Chen et al. [18], we start this study using 4-aminoquinazoline (**1a**), diethyl 4-cyclohexyl-2,6-dimethyl-1,4-dihydropyridine-3,5-dicarboxylate (**2a**), trifluoroacetic acid (TFA) and 2,2,2-trifluoroethanol (TFE) as solvent under blue LED irradiation for 4 h, followed by exposition to air to promote the rearomatization (Scheme 1). For our delight, the desired product **3a** was obtained in 57% yield (Table 1, Entry 1).

We then evaluated whether the amount of light delivered to the system influenced the reaction outcome. Using two 40 W LEDs (λ_{max} = 440 nm) resulted in a reduced yield of **3a** (13%, Table 1, Entry 2). Control experiments were performed to gain insight into the nature of the reaction. Light was found to be essential, as no formation of **3a** occurred in its absence (Table 1, Entry 3). The reaction was also sensitive to oxygen; exposing the system to air completely inhibited C–H functionalization (Table 1, Entry 4). Finally, the presence of acid proved crucial: without TFA, no product **3a** was detected (Table 1, Entry 5).

Next, we investigated the influence of reaction concentration. A more concentrated medium led to a decrease in yield (30%, Table 1, Entry 6). Conversely, dilution to 0.05 mol L^{-1} increased the yield to 74% (Table 1, Entry 7). Further dilution to 0.04 mol L^{-1}, however, again lowered the yield (61%, Table 1, Entry 8). Based on these results, a concentration of 0.05 mol L^{-1} was selected for subsequent studies. We also examined the amount of TFA required. Reducing TFA to 0.75 equiv. gave only traces of **3a** (Table 1, Entry 9), while increasing it to 2.0 equiv. decreased the yield to 55% (Table 1, Entry 10). Thus, the initial amount was maintained.

To determine whether a photocatalyst could enhance the reaction, we tested 1,2,3,5-tetrakis(carbazol-9-yl)-4,6-dicyanobenzene (4CzIPN), chosen for its long-lived excited state and favorable redox potentials ($E_1/_2(PC^*/PC^-)$ = +1.35 V *vs.* SCE) [19]. However, its use resulted in only 12% yield of **3a** (Table 1, Entry 11). Additional parameters—including acids, alternative light sources, and solvents—were screened in an effort to improve the transformation, but none afforded better results (see Supplementary Information).

With the optimal conditions established (Table 1, Entry 7), we next evaluated scalability. Performing the reaction on a 1 mmol scale afforded **3a** in 65% yield, allowing the isolation of 180.2 mg of product. We then examined the scope and limitations of the method (Scheme 1) and a variety of 4-alkyl-DHPs were evaluated. Functionalized products were obtained from unsaturated cyclic (**3b**, 35%) and saturated acyclic (**3c**, 41%) radical precursors. A DHP derived from ibuprofen also successfully afforded the C2-alkylated product **3d** in 33% yield. Recovery of unreacted starting material allowed a second alkylation cycle, providing **3d** in 76% combined yield. However, other 4-alkyl-DHPs failed to deliver the corresponding products **3e**–**3g**, probably due to insufficient stability of the generated radicals. Likewise, the DHP substituted with a tetrahydrofuran-3-yl group did not furnish the corresponding product **3h** (Scheme 1). Other DHPs were explored without success (see Supplementary Material).

Beyond the model substrate **1a**, a variety of quinazolines were examined. For instance, 4-methylquinazoline bearing substitution at the C8 position afforded the C2- alkylated product **3i** in 43% yield. For our delight, introduction of a chlorine atom into the radical acceptor improved the outcome, delivering product **3j** in 64% yield. Motivated by this result, a DHP substituted with 4-(tetrahydrofuran-3-yl) was evaluated in combination with 4-chloroquinazoline, providing the heteroatom-containing cyclic alkylated product **3k** in 24% yield. Therefore, the increase in electrophilicity of the heterocycle from **3h** to **3k**, due to the presence of an electron withdrawing chlorine atom, was able to sufficiently lower the LUMO energy to allow for the radical attack. This result suggests that the reaction does not depend solely on the stability and nucleophilicity of the radical.

To assess the versatility of the protocol, other heterocyclic scaffolds were also explored. Quinoxalin-2(1*H*)-one underwent successful C–H functionalization to give **3m** in 41% yield; however, *N*-alkylated analogue lead to traces of **3n** under the optimized conditions. The *N*-methyl group acts as an electron donor, effectively deactivating the heterocycle toward nucleophilic radical attack by decreasing the electrophilic character of the transient quinoxalinium species.

Pyrimidine was also amenable to alkylation, affording **3o** in 67% yield. Notably, to the best of our knowledge, photochemical C–H functionalization of unsubstituted pyrimidines at C2 has not been previously reported, with existing methods relying primarily on Grignard-based cross-coupling reactions [20]. We further examined substrates derived from natural products. Caffeine provided the alkylated product **3p** in 21% yield, while quinine derivative delivered **3q** in 71% yield.

Unsubstituted quinoline was also evaluated; however, the reaction resulted in a complex mixture from which no product could be isolated. GC-MS analysis of this mixture revealed two compounds with the *m/z* of

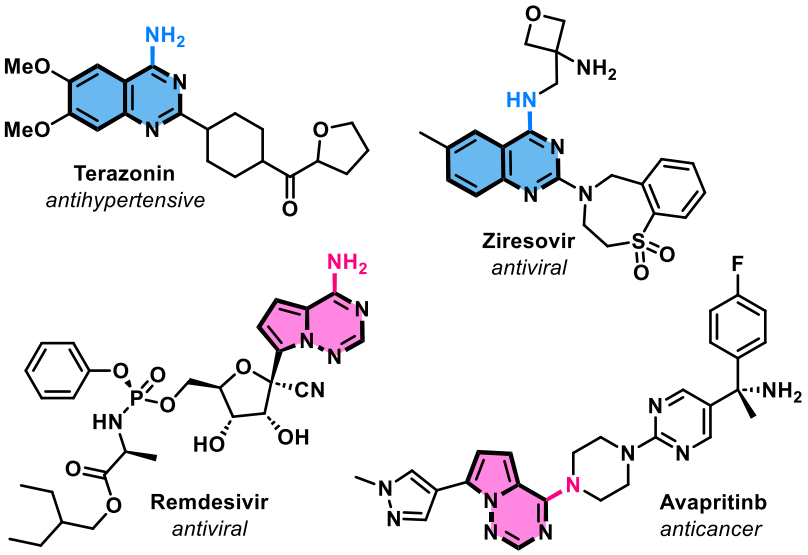

Fig. 1. Examples of drugs possessing 4-aminoquinazoline or pyrrolo[2,1-*f*][1,2,4]triazine core.

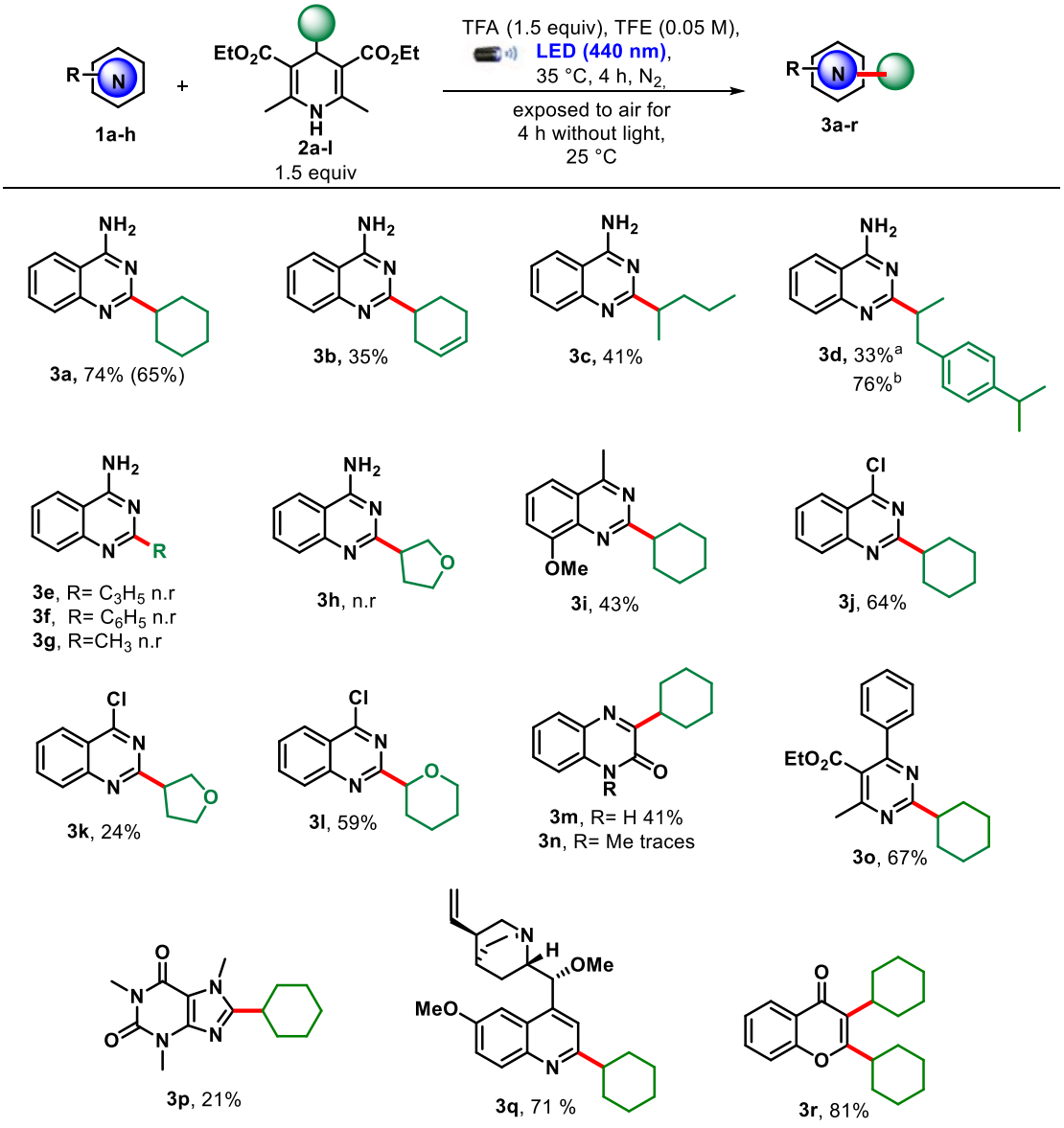

Scheme 1. Scope and limitations of the visible-light promoted C–H functionalization reaction. [a]first cycle of alkylation. [b]second cycle of alkylation.

the monoalkylated product. This suggests that alkylation likely occurred at the C2 and C4 positions. Under the acidic conditions of the reaction, protonation of the quinoline core increases the electrophilicity of these sites, thereby favoring the targeted alkylation (see Supplementary Material).

In addition, flavone—commonly found as a plant secondary metabolite [21] —underwent double alkylation to furnish **3r** in 81% yield. Additional heterocycles were also subjected to the photochemical C–H functionalization conditions; however, several substrates were not tolerated by the protocol (see Supplementary Material). Moreover, we have evaluated the compatibility of additional DHP classes within the protocol. When diethyl 4-(benzylcarbamoyl)-2,6-dimethyl-1,4-dihydropyridine-3,5-dicarboxylate was used as the radical precursor, no C2-functionalization product was observed and the starting quinazoline **1a** was recovered.

We next applied the developed protocol to the unnatural nitrogenous scaffold pyrrolo[2,1-*f*][1,2,4]triazine, the core structure of remdesivir, given its previously noted importance and synthetic challenges. For our delight, the corresponding C7-alkylated product **3s** was obtained in 10% yield, being its structure confirmed by single crystal X-ray analysis. To the best of our knowledge, this represents the first report of C7-functionalization of this nucleus without preactivation using a photochemical protocol. This result motivated further optimization efforts aimed at improving the yield of **3s** (Table 2).

Extending the reaction time in the first stage to 24 h resulted in a twofold increase in yield (Table 2, Entry 2). This suggested that a longer reaction period might be beneficial. However, conducting the reaction for 48 h led to degradation of the desired product (Table 2, Entry 3). Changing the light source was also evaluated, but no reaction occurred under these conditions (Table 2, Entry 4). Increasing the reaction concentration likewise did not improve the outcome (Table 2, Entry 5). Adjusting the amount of radical precursor proved unproductive as well, giving only traces of **3s** (Table 2, Entry 7). Notably, incorporating an additional lamp into the setup significantly improved the yield, providing **3s** in 31% yield (Table 2, Entry 8). Other polar solvents were explored, but without improvement in the process (Table 2, Entries 10 and 11).

With the optimized reaction conditions in hand (Table 2, Entry 8), we next examined the scope of DHPs to assess the robustness of the protocol (Scheme 2). Pyrrolo[2,1-*f*][1,2,4]triazine derivatives bearing

Table 1
Visible-light promoted C–H functionalization of 4-aminoquinazoline (**1a**) with Hantzsch ester **2a**.

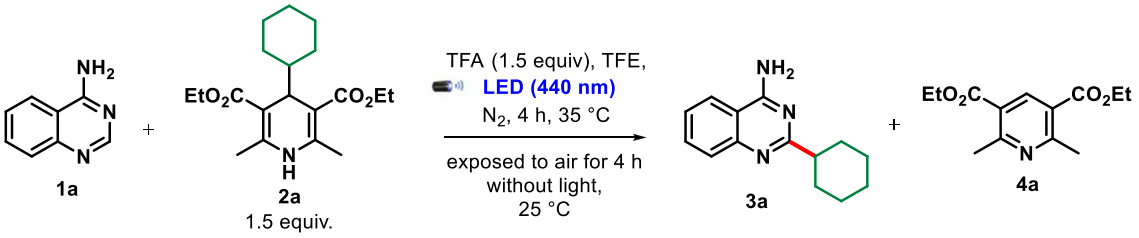

Entry	Variation	Yield 3a (%)[c]
1[a]	None	57
2	2 LEDs (40 W each)	13
3	Absence of light throughout the process	n.r[d]
4	Air exposure throughout the method	n.r[d]
5	Absence of acid	n.r[d]
6	Concentration 0.1 → 0.2 mol L^{-1}	30
7[b]	**Concentration 0.1 → 0.05 mol L^{-1}**	**74**
8	Concentration 0.1 → 0.04 mol L^{-1}	61
9[b]	0.75 equiv. TFA	traces
10[b]	2.0 equiv. TFA	55
11[b]	4CzIPN (1 mol%)	12

[a] reaction carried out in a 10 mL Schlenk flask, under a N_2 atmosphere, containing **1a** (0.2 mmol; 1.0 equiv.), **2a** (0.3 mmol; 1.5 equiv.), TFA (0.3 mmol; 1.5 equiv.) and TFE (2 mL), irradiating with a 40 W Kessil LED ($\lambda_{max.}$ = 440 nm). Performing freeze-pump-thaw (3 cycles).
[b] Using TFE (4 mL).
[c] Isolated yields after purification by column chromatography.
[d] n.r = no reaction.

Table 2
Optimization of functionalization of pyrrolo[2,1-*f*][1,2,4]triazine.

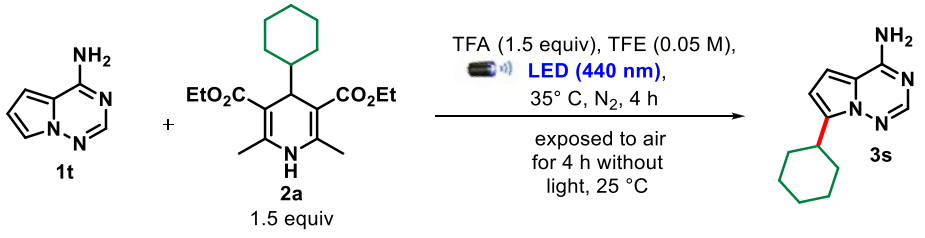

Entry	Variation	3s, Yield (%)[b]
1[a]	None	10
2	24 h in the first stage	20
3	48 h in the first stage	n.d[c]
4	$\lambda_{max.}$ = 390 nm P = 40 W	n.r[d]
5	TFE (1 mL)	traces
6	TFE (3 mL)	13
7	3.0 equiv. of **2a**	traces
8	**2 LEDs (40 W each)**	**31**
9	36 h in the first stage	29
10	HFIP[e]	traces
11	DMSO	10

[a] reaction carried out in a 10 mL Schlenk flask, under a N_2 atmosphere, containing **1t** (0.10 mmol; 1.0 equiv.), **2a** (0.15 mmol; 1.5 equiv.), TFA (0.15 mmol; 1.5 equiv.) and TFE (2 mL), irradiating with a 40 W Kessil LED ($\lambda_{max.}$ = 440 nm). Performing freeze-pump-thaw (3 cycles).
[b] Isolated yields after purification by column chromatography.
[c] n.d = not determined, degradation of reaction components.
[d] n.r = no reaction.
[e] HFIP = 1,1,1,3,3,3-hexafluoroisopropanol.

cyclohexenyl (**3t**), 2-pentyl (**3u**), and ibuprofen-derived (**3v**) substituents were obtained in yields of up to 26% (Scheme 2). Notably, in all cases, exclusive C7-alkylation was observed.

Vrabel et al. reported that alkylation of 1,2,4-triazines occurs selectively at the *N*1 position, affording *N*1-alkyl triazinium salts [22], which suggests that this nitrogen atom is the most nucleophilic and best able to stabilize positive charge. By analogy, we propose that the regioselectivity observed in the C7-alkylation of pyrrolo[2,1-*f*][1,2,4]

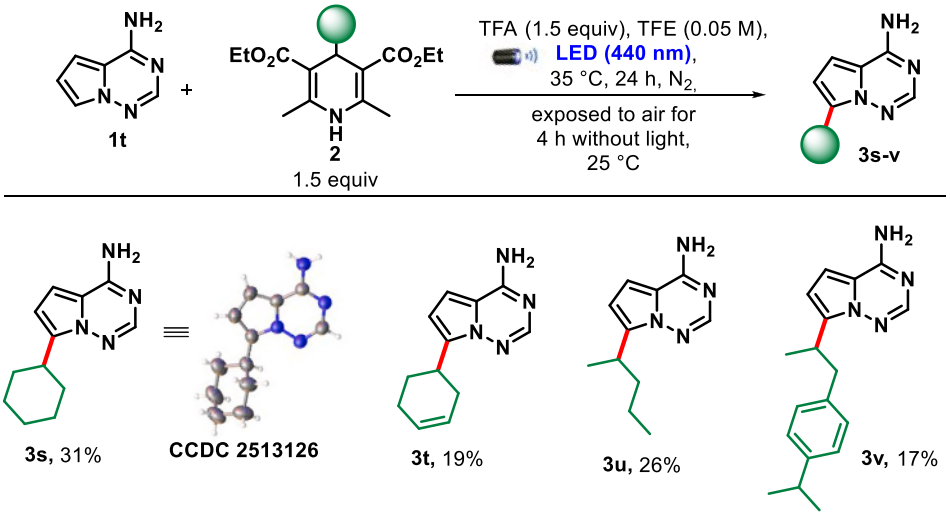

Scheme 2. Alkylation of pyrrolo[2,1-*f*][1,2,4]triazine.

triazine arises from preferential stabilization of the positive charge, upon protonation with TFA, by the nitrogen at the 7a instead of at the 1 position (see Supplementary Material). Therefore, the C7-alkylation would be in agreement with the Minisci aryl substitutions [23].

With regard to the mechanism of the studied reaction, further experiments were conducted to supplement the discussions already reported [18]. With this, we began our investigations with UV-Vis studies of the starting material **1a** and the radical precursor **2a** in conjunction with TFA (see Supplementary Material). Upon analysis of these results, no bathochromic shift of the mixture was observed, which may indicate that the reaction does not occur using an electron donor-acceptor (EDA) complex [24,25] but rather by direct excitation of the radical precursor **2a**.

Further evidence was gathered by studying the NMR of both initial components individually in the same solvent and then the mixture of both (see Supplementary Material). By observing the NMR spectra, it can be seen that the chemical shifts of the initial materials individually and when arranged in a mixture are the same, indicating that the EDA complex is not formed in this protocol.

Simultaneously with these analyses, studies were conducted with radical scavengers. Thus, the reaction was carried out under optimized conditions with the addition of the radical scavenger 2,2,6,6-tetramethylpiperidine-1-yl)oxyl (TEMPO). At the end of the reaction period, it was not possible to observe the formation of the functionalized product at C-2 (**3a**) using TLC analysis, thus suggesting that the radical species present in the reaction mixture may have been captured by the sequestering agent added to the reaction medium. This fact was confirmed by analyzing the full scan mass spectrum, which is consistent with previously reported data [18] (see Supplementary Material). We have also monitored the reaction every 2 h by direct infusion mass spectrometry (DI-MS), and it was possible to detect the unoxidized product **IV** (see Supplementary Material).

In addition, experiments were conducted by alternating light exposure to the system. When analyzing the results (see Supplementary Material), it can be understood that constant irradiation is necessary to obtain **3a**, since during the periods when the light was turned off, the yield remained constant. This shows that the alkyl radical present in the medium may be a transient radical and, consequently, no parallel reactions occur. Considering the evidence presented and what is reported in the literature, Scheme 3 shows a proposed mechanism for the C–H

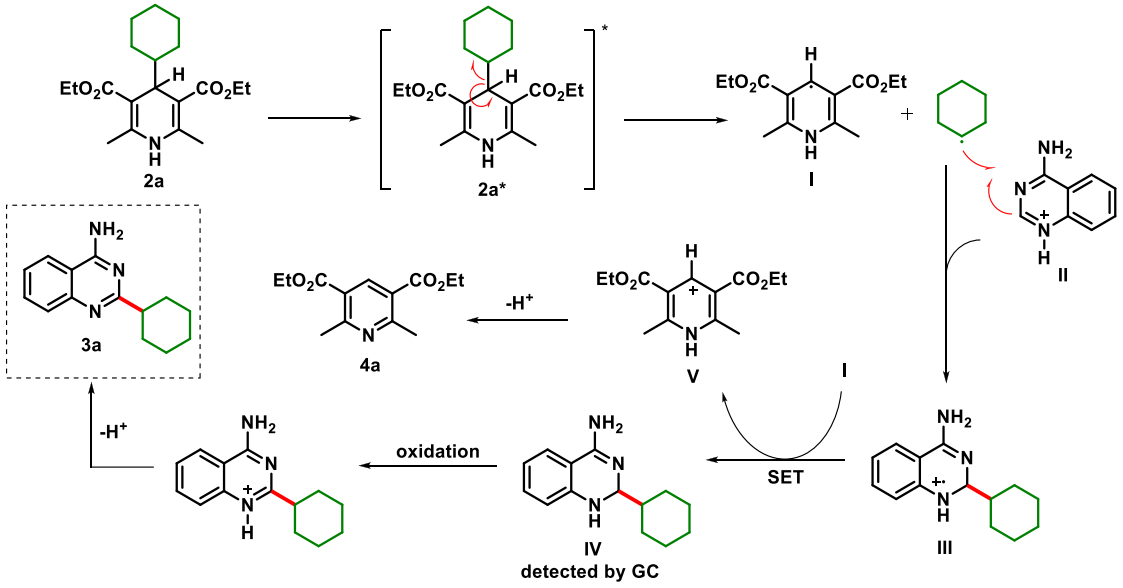

Scheme 3. Proposed mechanism for the C–H functionalization reaction of **1a**.

functionalization of **1a**.

Initially, DHP **2a** absorbs visible light and is promoted to its electronically excited state **2a***, which undergoes homolytic cleavage to generate the alkyl radical. The resulting radical then adds to the protonated 4-aminoquinazoline **II** [26] via a Minisci-type nucleophilic aromatic substitution, affording radical cation intermediate **III**. Subsequently, a single-electron transfer (SET) between intermediates **I** and **III** furnishes intermediate **IV**, which is further oxidized by molecular oxygen present in the reaction medium to deliver the protonated alkylated product. The aromatized DHP derivative **4a** is formed as a byproduct of the process.

3. Conclusion

In conclusion, an oxidant- and photocatalyst-free protocol was developed for the C–H functionalization of quinazolines, furnishing 8 derivatives in 24–76% yield. Moreover, late-stage functionalization of bioactive natural products, such as caffeine, quinine derivative and flavone was carried out. Notably, the protocol enabled the selective C7-functionalization of the pyrrolo[2,1-*f*][1,2,4]triazine core without the need for pre-functionalization, representing the first example of such a transformation achieved through a photochemical process. Exploratory studies aimed at improving the C7- alkylation revealed a maximum yield of 31% to date. Given the synthetic relevance of this transformation, further optimization of the protocol is ongoing, including efforts to access more structurally complex derivatives.

4. Methods and materials

4.1. General information

Commercially available reagents were purchased from Merck, and when necessary, additional purifications were carried out as reported in the literature. The synthesized products were purified through a chromatographic column using flash silica gel 60 Å, 230–400 mesh. The thin layer chromatography (TLC) was performed in silica gel 60 F_{254} supported in aluminum sheets. The Nuclear Magnetic Resonance (NMR) ^{1}H and $\{^{1}H\}^{13}C$ NMR spectra were recorded on a Bruker DRX 400 MHz spectrometer. Chemical shifts (δ) were presented in ppm units and the coupling constants (*J*) in Hertz (Hz). Abbreviations were used to express the multiplicity of signals: s (singlet), d (doublet), t (triplet), q (quartet), m (multiplet). The reactions conducted under microwave irradiation were carried out in a CEM Discovery®. Melting points were recorded with a digital fusometer (Büchi, M − 560) and were expressed in degrees Celsius (°C). The photochemical reactions were carried out in a 10 mL Schlenk flask which was irradiated by a 40 W Kessil H1160L blue LED with a maximum emission of 440 nm. The LED was positioned 3 cm from the Schlenk flask. UV/Vis detection analyses were performed in a 1.0 cm quartz cuvette using a Shimadzu model 1800 UV/Vis spectrophotometer at 20 °C. Absorption spectra of the individual components were obtained at the same concentration as the reaction under study. Complete scan mass spectra of the crude reaction product were obtained on a Waters Xevo TQD triple quadrupole mass spectrometer. Single-crystal X-ray diffraction studies were conducted at room temperature using a Rigaku XtaLAB Synergy-S Dualflex diffractometer, equipped with a HyPix-6000HE detector system and CuKα radiation (λ = 1.54184 Å). HRMS-ESI analyses were conducted on an Agilent 6545 qTOFMS spectrometer (Agilent Technologies, Santa Clara, CA, USA) with an electrospray interface (ESI) in positive mode. The GC-MS analyses were conducted using a Shimadzu GCMS-QP2010S instrument with electron impact ionization (EI) using a Zebron-ZB-5MS column.

4.2. General procedure for photochemical alkylation of heterocycles

In a 10 mL Schlenk tube, the heterocycle (**1a-z**) (0.2 mmol; 1.0 equiv.), the radical precursor of interest (**2a-m**) (1.5 equiv.), and 2,2,2-trifluoroethanol (4 mL) were added. Subsequently, the freeze-pump-thaw cycle (3 cycles) was performed on the system and, with the aid of a syringe, TFA (0.3 mmol; 23.1 μL) was added to the reaction system. The Schlenk was positioned in front of a 40 W Kessil H1160L blue LED with a maximum emission of 440 nm, allowing it to be irradiated for 4 h. The system also remained under constant agitation during this period. At the end of this period, the Schlenk was opened and the LED turned off, and the reaction system continued to be stirred for another 4 h. At the end of the reaction period, Et_3N (69 μL; 0.43 mmol) was added. The reaction mixture was then evaporated at reduced pressure and subsequently purified on a flash chromatography column 18.

2-Cyclohexyl-4-quinazolinamine (**3a**) 27: The product was purified on a gradient of 30–70% EtOAc:hexane, with the column doped with 1% Et_3N. The product was obtained as a white solid with a 74% yield (33.6 mg, 0.14 mmol). mp: 228-231 °C (lit. 230-232 °C) [27]. ^{1}H NMR (400 MHz, DMSO-d_6) *δ*: 9.70 (d, *J* = 35.1 Hz, 2H), 8.41 (d, *J* = 8.2 Hz, 1H), 8.02 (t, *J* = 7.7 Hz, 1H), 7.81 (d, *J* = 8.3 Hz, 1H), 7.71 (t, *J* = 7.7 Hz, 1H), 2.86 (ddd, *J* = 11.7, 8.6, 3.3 Hz, 1H), 1.95 (d, *J* = 11.9 Hz, 2H), 1.83 (d, *J* = 13.0 Hz, 2H), 1.74 – 1.68 (m, 1H), 1.66 – 1.54 (m, 2H), 1.35 (dd, *J* = 25.5, 12.7 Hz, 2H), 1.29 – 1.13 (m, 1H). $^{13}C\{^{1}H\}$ NMR (100 MHz, DMSO-d_6) *δ*: 167.7, 164.0, 139.4, 136.7, 128.1, 125.3, 119.4, 111.6, 44.0, 30.6, 25.6. HRMS (ESI$^+$): *m/z* calcd for: $C_{14}H_{17}N_3$ $[(M + H)]^+$: 228.1500; found: 228.1509.

2,6-Dimethyl-3,5-pyridinedicarboxylic acid diethyl ester (**4a**) 28: The compound was purified with 30% EtOAc:Hexane as the mobile phase. The compound was obtained as a white solid. The yield of this by-product was not determined. mp: 68-72 °C (lit. 66-68 °C) [28]. ^{1}H NMR (400 MHz, $CDCl_3$) *δ*: 8.77 (s, 1H), 4.40 (q, *J* = 7.1 Hz, 4H), 2.89 (s, 6H), 1.41 (t, *J* = 7.1 Hz, 6H). $^{13}C\{^{1}H\}$ NMR (100 MHz, $CDCl_3$) *δ*: 165.2, 161.7, 142.0, 123.8, 61.7, 23.8, 14.2.

4-(Benzylcarbamoyl)-2,6-dimethylpyridine-3,5-dicarboxylate diethyl ester (**4b**): The product was purified with 30% EtOAc:Hexane as the mobile phase. The product was obtained as a yellow oil. The yield of this by-product was not determined. ^{1}H NMR (400 MHz, $CDCl_3$) *δ*: 7.30 – 7.19 (m, 5H), 6.40 (brs, 1H), 4.45 (d, *J* = 5.8 Hz, 2H), 4.13 (q, *J* = 7.1 Hz, 4H), 2.51 (s, 6H), 1.19 (t, *J* = 7.1 Hz, 3H).

2-Cyclohex-3-en-1-yl)*quinazolin-4-amine* (**3b**): The product was purified on a gradient of 30–50% EtOAc:hexane, with the column doped with 1% Et_3N. The product was obtained as a solid yellow with a 35% yield (15.7 mg, 0.06 mmol). mp: 186-190 °C. ^{1}H NMR (400 MHz, DMSO-d_6) *δ*: 8.16 (d, *J* = 8.2 Hz, 1H), 7.72-7.59 (m, 4H), 7.40 (t, *J* = 7.5 Hz, 1H), 5.74 (dd, *J* = 22.6, 11.7 Hz, 2H), 2.81 (t, *J* = 12.3 Hz, 1H), 2.44 (d, *J* = 11.2 Hz, 1H), 2.25 (d, *J* = 17.4 Hz, 1H), 2.12 (s, 2H), 2.00 (d, *J* = 12.6 Hz, 1H), 1.84 – 1.67 (m, 1H). $^{13}C\{^{1}H\}$ NMR (100 MHz, DMSO-d_6) *δ*: 170.0, 162.4, 150.6, 133.0, 127.6, 127.1, 126.9, 125.0, 123.9, 113.4, 43.3, 30.2, 28.2, 25.6. HRMS (ESI$^+$): *m/z* calcd for: $C_{14}H_{15}N_3$ $[(M + H)]^+$: 226.1344; found: 226.1349.

2-(1-Methylbutyl)-4-quinazolinamine (**3c**) 27: The product was purified with a gradient of 30-70% EtOAc: Hexane, with the column doped with 1% Et_3N. The product was obtained as a white solid with a 41% yield. (17.6 mg, 0.08 mmol). mp: 161-165 °C (lit. 162-164 °C) [15].^{1}H NMR (400 MHz, DMSO-d_6) *δ*: 8.15 (dd, *J* = 8.2, 0.7 Hz, 1H), 7.71 – 7.58 (m, 4H), 7.38 (ddd, *J* = 8.1, 6.9, 1.2 Hz, 1H), 2.78 (dd, *J* = 14.6, 6.8 Hz, 1H), 1.88 – 1.73 (m, 1H), 1.52 – 1.40 (m, 1H), 1.20 (dd, *J* = 9.9; 4.7 Hz, 4H), 0.83 (t, *J* = 7.3 Hz, 3H). $^{13}C\{^{1}H\}$ NMR (100 MHz, DMSO-d_6) *δ*: 170.8, 162.4, 150.6, 132.9, 127.5, 124.8, 123.8, 113.4, 42.8, 38.4, 20.8, 20.3, 14.6.

2-(1-(4-Isopropylphenyl)propan-2-yl)*quinazolin-4-amine* (**3d**): The product was purified with a gradient of 30-70% EtOAc:Hexane, with the column doped with 1% Et_3N. The product was obtained as a yellow oil with a 33% yield. (20.1 mg, 0.06 mmol). ^{1}H NMR (400 MHz, DMSO-d_6) *δ*: 8.14 (d, *J* = 7.6 Hz, 1H), 7.74 – 7.58 (m, 4H), 7.40 (dd, *J* = 11.0, 4.0 Hz, 1H), 7.07 (s, 4H), 3.20 – 3.12 (m, 1H), 3.04 (d, *J* = 7.1 Hz, 1H), 2.83 – 2.66 (m, 2H), 1.18-1.12 (m, 9H). $^{13}C\{^{1}H\}$ NMR (100 MHz, DMSO-d_6) *δ*: 170.3, 162.5, 150.4, 146.0, 138.8, 133.2, 129.3, 127.5, 126.5, 125.2, 123.9, 113.4, 44.9, 41.3, 33.5, 24.5, 24.4, 19,9. HRMS (ESI$^+$): *m/z* calcd

for: $C_{20}H_{23}N_3$ [(M + H)]$^+$: 305.1892; found: 306.1968.

4-Methyl-7-methoxy-2-cyclohexylquinazoline (**3i**): The product was purified with 20% EtOAc: Hexane as the mobile phase. The product was obtained as a yellow oil with a 43% yield. (22.0 mg, 0.08 mmol). ^{1}H NMR (400 MHz, $CDCl_3$) δ: 6.85 (d, J = 7.9 Hz, 1H), 6.70 (d, J = 7.8 Hz, 1H), 6.53 (t, J = 7.9 Hz, 1H), 3.76 (s, 3H), 2.24 (s, 3H), 1.86-1.83 (m, 2H), 1.71-1.59 (m, 10H).

4-Chloro-2-cyclohexylquinazoline (**3j**) 29: The product was purified with EtOAc: Hexane 2:8 as the mobile phase. The product was obtained as a white solid with a 64% yield (31.5 mg, 0.12 mmol). mp: 208-211 °C. ^{1}H NMR (400 MHz, $CDCl_3$) δ: 8.29 (dd, J = 8.0, 1.1 Hz, 1H), 7.78 – 7.70 (m, 2H), 7.46 (ddd, J = 8.1, 7.0, 1.4 Hz, 1H), 2.77 – 2.71 (m, 1H), 2.09 – 2.01 (m, 2H), 1.96 – 1.88 (m, 2H), 1.83 – 1.71 (m, 3H), 1.52 – 1.38 (m, 3H). ^{13}C{^{1}H} NMR (100 MHz, $CDCl_3$) δ: 164.2, 160.2, 149.6, 134.7, 127.4, 126.3, 126.2, 120.8, 44.9, 30.5, 26.0, 25.7.

4-Chloro-2-(tetrahydro-3-furanyl)quinazoline (**3k**): The product was purified with EtOAc: Hexane 3:7 as the mobile phase. The product was obtained as a white solid with a 24% yield. (11.2 mg, 0.04 mmol). mp: 252-256 °C. ^{1}H NMR (400 MHz, $CDCl_3$) δ: 8.27 (d, J = 7.9 Hz, 1H), 7.77 (t, J = 7.6 Hz, 1H), 7.69 (d, J = 8.1 Hz, 1H), 7.48 (t, J = 7.5 Hz, 1H), 4.23 – 4.17 (m, 2H), 4.08 – 4.04 (m, 1H), 3.94 – 3.88 (m, 1H), 3.58 – 3.49 (m, 1H), 2.54 – 2.46 (m, 1H), 2.39 – 2.31 (m, 1H). ^{13}C{^{1}H} NMR (100 MHz, $CDCl_3$) δ: 163.2, 157.1, 148.8, 134.9, 126.8, 126.4, 120.9, 71.5, 68.1, 44.6, 31.3.

*4-Chloro-2-(tetrahydro-2H-pyran-*2-yl*)quinazoline* (**3l**): The product was purified with EtOAc: Hexane 3:7 as the mobile phase. The product was obtained as a white solid with a 59% yield (15.0 mg, 0.06 mmol). mp: 129-130 °C. ^{1}H NMR (400 MHz, $CDCl_3$) δ: 8.28 (d, J = 7.9 Hz, 1H), 7.75 (t, J = 7.6 Hz, 1H), 7.65 (d, J = 8.1 Hz, 1H), 7.46 (t, J = 7.5 Hz, 1H), 4.38 (dd, J = 11.1, 2.0 Hz, 1H), 4.23 – 4.15 (m, 1H), 3.64 (td, J = 10.6, 3.0 Hz, 1H), 2.26 (d, J = 14.1 Hz, 1H), 2.01-1.99 (m, 1H), 1.58-1.51 (m, 2H), 1.30-1.25 (m, 2H). ^{13}C{^{1}H} NMR (100 MHz, $CDCl_3$) δ: 161.5, 155.8, 148.9, 134.6, 127.1, 126.6, 121.5, 76.0, 68.0, 30.1, 25.4, 22.9.

3-Cyclohexyl-2(1H)-quinoxalinone (**3m**) 30: The product was purified with EtOAc: Hexane 2:8 as the mobile phase. The product was obtained as a white solid with a 41% yield. (18.7 mg, 0.08 mmol). mp: 252-253 °C (lit. 252-253 °C) [30]. ^{1}H NMR (400 MHz, $CDCl_3$) δ: 10.85 (brs, 1H), 7.83 (d, J = 8.0 Hz, 1H), 7.46 (t, J = 7.6 Hz, 1H), 7.32 (t, J = 7.6 Hz, 1H), 7.28 – 7.22 (m, 1H), 3.34 (t, J = 11.3 Hz, 1H), 1.99 (d, J = 12.2 Hz, 2H), 1.89 (d, J = 12.6 Hz, 2H), 1.79 (d, J = 12.6 Hz, 1H), 1.56-1.47 (m, 3H), 1.40 – 1.23 (m, 2H). ^{13}C{^{1}H} NMR (100 MHz, $CDCl_3$) δ: 165.0, 155.6, 132.9, 130.6, 129.5, 129.0, 123.9, 115.1, 40.2, 30.5, 26.3, 26.1.

Ethyl 2-cyclohexyl-4-methyl-6-phenyl-5-pyrimidinecarboxylate (**3o**) 11: The product was purified with EtOAc: Hexane 1:9 as the mobile phase. The product was obtained as a yellow oil with a 67% yield (43.4 mg, 0.13 mmol). ^{1}H NMR (400 MHz, $CDCl_3$) δ: 7.63 (dd, J = 7.8, 1.8 Hz, 2H), 7.47 – 7.40 (m, 3H), 4.15 (q, J = 7.1 Hz, 2H), 3.93-3.86 (m, 1H), 2.55 (s, 3H), 1.81 – 1.77 (m, 3H), 1.64 – 1.55 (m, 3H), 1.49 – 1.45 (m, 1H), 1.42 – 1.37 (m, 2H), 1.33 – 1.28 (m, 1H). ^{13}C{^{1}H} NMR (100 MHz, $CDCl_3$) δ: 172.8, 168.7, 166.0, 164.0, 138.3, 130.5, 128.9, 128.8, 121.2, 62.1, 44.2, 33.3, 26.4, 26.2, 23.1, 14.1. HRMS (ESI$^+$): *m/z* calcd for: $C_{20}H_{24}N_2O_2$ [(M + H)]$^+$: 325.1916; found: 325.1923.

8-Cyclohexylcaffeine (**3p**) 31: The product was purified with EtOAc: Hexane 3:7 as the mobile phase. The product was obtained as a white solid with a 21% yield (11.6 mg, 0.04 mmol). MP: 209-210 °C (lit. 207-209 °C) [31]. ^{1}H NMR (400 MHz, $CDCl_3$) δ: 3.92 (s, 3H), 3.57 (s, 3H), 3.39 (s, 3H), 2.70 (ddd, J = 11.7, 8.3, 3.4 Hz, 1H), 1.92 – 1.83 (m, 4H), 1.79 – 1.59 (m, 3H), 1.45 – 1.32 (m, 3H). ^{13}C{^{1}H} NMR (100 MHz, $CDCl_3$) δ: 158.0, 155.5, 151.8, 148.1, 107.0, 35.8, 31.4, 30.9, 29.7, 27.8, 26.0, 25.6. HRMS (ESI$^+$): *m/z* calcd for: $C_{14}H_{20}N_4O_2$ [(M + H)]$^+$: 277.1665; found: 277.1665.

*(1S,2S,4S,5R)-2-((R)-(2-Cyclohexyl-6-methoxyquinolin-*4-yl*)(methoxy)methyl)-5-vinylquinuclidine* (**3q**) 32: The product was purified with EtOAc:MeOH (8:2), with the column doped with 1% Et_3N. The product was obtained as a yellow oil with a 71% yield (57.7 mg, 0.13 mmol). ^{1}H NMR (400 MHz, $CDCl_3$) δ: 7.98 (d, J = 9.2 Hz, 1H), 7.44 (s, 1H), 7.38 – 7.35 (m, 2H), 6.26 (s, 1H), 5.58 (ddd, J = 17.1, 10.3, 6.9 Hz, 1H), 5.08 – 5.04 (m, 2H), 4.11 (s, 3H), 3.47 (s, 3H), 3.36 (t, J = 8.9 Hz, 1H), 3.22 – 3.18 (m, 1H), 3.11 (d, J = 13.4 Hz, 1H), 2.91 – 2.84 (m, 1H), 2.71 (s, 1H), 2.30 (s, 1H), 2.15 (d, J = 13.2 Hz, 3H), 2.00 (d, J = 12.5 Hz, 2H), 1.89 (d, J = 12.1 Hz, 3H), 1.81 – 1.74 (m, 2H), 1.60 (dd, J = 24.7, 12.5 Hz, 2H), 1.47 (dd, J = 25.0, 12.4 Hz, 3H), 1.32 (ddd, J = 23.3, 16.0, 6.2 Hz, 3H). ^{13}C{^{1}H} NMR (100 MHz, $CDCl_3$) δ: 161.9, 160.0, 137.0, 127.0, 126.2, 125.9, 117.7, 116.6, 100.4, 59.2, 57.4, 57.2, 54.3, 44.3, 43.8, 36.9, 32.8, 32.7, 30.9, 26.9, 26.0, 25.6, 24.3, 18.8,

2,3-Dicyclohexyl-4H-chromen-4-one (**3r**): The product was purified with EtOAc: Hexane 1:9 as the mobile phase. The product was obtained as a yellow oil with an 81% yield (37.5 mg, 0.12 mmol). ^{1}H NMR (400 MHz, $CDCl_3$) δ: 7.87 – 7.85 (m, 1H), 7.48 – 7.44 (m, 1H), 7.00 – 6.95 (m, 2H), 4.20 (ddd, J = 9.4, 5.6, 3.3 Hz, 2H), 2.77 – 2.62 (m, 2H), 1.99 (d, J = 12.3 Hz, 1H), 1.81 (d, J = 13.0 Hz, 4H), 1.74 (dd, J = 14.5, 7.8 Hz, 4H), 1.60 (s, 2H), 1.40 – 1.36 (m, 1H), 1.30 – 1.26 (m, 2H), 1.16 (dd, J = 24.2, 11.8 Hz, 3H). ^{13}C{^{1}H} NMR (100 MHz, DMSO-d_6) δ: 193.1, 161.2, 135.9, 126.9, 121.0, 117.9, 82.0, 41.8, 40.3, 28.3, 28.2, 26.3, 26.0, 26.9.

7-cyclohexylpyrrole[2,1-f][1,2,4]triazine (**3s**): The product was purified on a preparative plate using EtOAc: Hexane 6:4 as the eluent. The product was obtained as a white solid with a 31% yield (6.7 mg, 0.03 mmol). MP: 203-206 °C. ^{1}H NMR (400 MHz, DMSO-d_6) δ: 7.79 (s, 1H), 7,54 (brs, 2H), 6.79 (d, J = 4.4 Hz, 2H), 6.39 (d, J = 4.3 Hz, 1H), 3.06 (s, 1H), 1.98 (d, J = 6.5 Hz, 2H), 1,75 (dd, J = 24.9, 9.3 Hz, 4H), 1.39 (t, J = 9.9 Hz, 4H). ^{13}C{^{1}H} NMR (100 MHz, DMSO-d_6) δ: 156.1, 147.9, 136.0, 114.1, 107.0, 101.1, 34.5, 31.8, 26.4, 26.2. HRMS (ESI$^+$): *m/z* calcd for: $C_{12}H_{16}N_4$ [(M + H)]$^+$: 217.1453; found: 217.1459.

*7-(cyclohex-3-en-*1-yl*)pyrrolo[2,1-f][1,2,4]triazin-4-amine* (**3t**): The product was purified with EtOAc: Hexane 3:7 as the mobile phase. The product was obtained as a white solid with an 19% yield (8.0 mg, 0.03 mmol). ^{1}H NMR (400 MHz, DMSO-d_6) δ: ^{1}H NMR (400 MHz, DMSO) δ 7.81 (s, 2H), 6.86 (d, J = 4.3 Hz, 1H), 6.43 (d, J = 4.3 Hz, 1H), 5.69 (s, 2H), 2.33 (d, J = 15.9 Hz, 1H), 2.15 – 2.09 (m, 2H), 2.03 (s, 1H), 1.99 – 1.93 (m, 2H), 1.64 (ddd, J = 23.4, 11.4, 5.7 Hz, 1H). ^{13}C{^{1}H} NMR (100 MHz, DMSO-d_6) δ: 154.9, 146.2, 136.2, 127.2, 126.5, 113.8, 107.9, 102.6, 30.6, 30.2, 27.5, 25.2. HRMS (ESI$^+$): *m/z* calcd for: $C_{12}H_{14}N_4$ [(M + H)]$^+$: 215.1297; found: 215.1299.

*7-(pentan-*2-yl*)pyrrolo[2,1-f][1,2,4]triazin-4-amine* (**3u**): The product was purified with EtOAc: Hexane 3:7 as the mobile phase. The product was obtained as a white solid with an 26% yield (11.0 mg, 0.05 mmol). ^{1}H NMR (400 MHz, DMSO-d_6) δ: 7.85 (s, 1H), 7.78 (brs, 1H), 6.90 (d, J = 4.4 Hz, 1H), 6.45 (d, J = 4.3 Hz, 1H), 3.33 (dd, J = 14.0, 7.0 Hz, 2H), 1.74 – 1.66 (m, 1H), 1.61 – 1.49 (m, 1H), 1.24 (d, J = 6.8 Hz, 3H), 0.84 (t, J = 7.3 Hz, 3H). ^{13}C{^{1}H} NMR (100 MHz, DMSO-d_6) δ: 115.1, 146.5, 136.9, 113.7, 107.7, 102.4, 38.0, 29.6, 20.4, 19.9, 14.4. HRMS (ESI$^+$): *m/z* calcd for: $C_{11}H_{16}N_4$ [(M + H)]$^+$: 205.1454; found: 205.1450.

*7-(1-(4-isopropylphenyl)propan-*2-yl*)pyrrolo[2,1-f][1,2,4]triazin-4-amine* (**3v**): The product was purified with EtOAc: Hexane 3:7 as the mobile phase. The product was obtained as a white solid with an 17% yield (10.0 mg, 0.03 mmol). MP: 100-101 °C. ^{1}H NMR (400 MHz, DMSO-d_6) δ: 7.82 (s, 1H), 7.55 (brs, 2H), 7.07 (dd, J = 18.8, 8.0 Hz, 4H), 6.80 (d, J = 4.3 Hz, 1H), 6.44 (d, J = 4.3 Hz, 1H), 3.64 – 3.49 (m, 1H), 3.08 (dd, J = 13.4, 6.2 Hz, 1H), 2.86 – 2.77 (m, 1H), 2.76 – 2.69 (m, 1H), 1.19 – 1.15 (m, 9H). ^{13}C{^{1}H} NMR (100 MHz, DMSO-d_6) δ: 156.0, 148.0, 146.2, 138.0, 135.2, 129.3, 126.4, 114.3, 107.7, 101.1, 33.4, 32.0, 24.4, 19.1. HRMS (ESI$^+$): *m/z* calcd for: $C_{18}H_{22}N_4$ [(M + H)]$^+$: 295.1923; found: 295.1928.

4.3. Scale-up experiment

In 100 mL Schlenk flask, 4-aminoquinazoline (**1a**) (1.0 mmol, 145.1 mg), the radical precursor (**2a**) (1.5 equiv.) and TFE (20 mL) were added. Subsequently, the freeze-pump-thaw cycle (3 cycles) was performed, and then TFA (1.5 mmol; 115.5 μL) was added to the reaction system. The Schlenk was positioned 3 cm from a 40 W Kessil H1160L blue LED with a maximum emission of 440 nm, allowing it to be

irradiated for 4 h. The system also remained under constant stirring during this period. After this time, the Schlenk was opened and the LED turned off, and the reaction continued under stirring for another 4 h. At the end of this period, Et_3N (345 μL; 2.15 mmol) was added. The reaction mixture was then evaporated under reduced pressure and subsequently purified on a flash chromatography column on a gradient of 30–70% EtOAc:hexane, with the column doped with 1% Et_3N. The product **3a** was obtained as a white solid with a 65% yield (180 mg, 0.65 mmol).

4.4. Radical scavenger experiment

A reaction was carried out under the optimal conditions obtained in the optimization process (Table 1, Entry 7), with the addition of 3.0 equiv. of the radical scavenger 2,2,6,6-tetramethylpiperidine-1-yl)oxyl (TEMPO). At the end of the reaction period Et_3N (69 μL; 0.43 mmol) was added to the crude reaction mixture, which was subsequently concentrated under reduced pressure. An aliquot was removed from the crude reaction and a sample was prepared in 1% HCOOH/MeOH and analyzed by mass spectrometry using an ACQUITY UPC2-MS apparatus through direct infusion (see Supplementary Material).

CRediT authorship contribution statement

Jhonathan R.N. dos Santos: Writing – review & editing, Writing – original draft, Methodology, Investigation, Formal analysis, Data curation, Conceptualization. **Victor Biagio A. Sciota:** Methodology, Investigation, Formal analysis. **Geovana F. Vargas:** Methodology, Investigation. **Camila Batista Pinto:** Methodology. **Giovanni W. Amarante:** Writing – review & editing, Writing – original draft, Conceptualization. **Javier Ellena:** Formal analysis. **Arlene G. Corrêa:** Writing – review & editing, Writing – original draft, Supervision, Funding acquisition, Formal analysis, Conceptualization.

Declaration of generative AI and AI-assisted technologies in the writing process

During the preparation of this work, the authors used Chat Generative Pre-Trained Transformer (ChatGPT; OpenAI, San Francisco, CA, USA) to enhance readability and language, aiding in formulating and structuring content. After using this tool, the authors reviewed and edited the content as needed and take full responsibility for the content of the publication.

Declaration of competing interest

The authors declare that they have no known competing financial interests or personal relationships that could have appeared to influence the work reported in this paper.

Acknowledgements

The authors acknowledge FAPESP (2014/50918–7, 2016/20609-8, 2017/15850-0, 2021/12394-0), GlaxoSmithKline, CAPES (Finance Code 001) and CNPq (312505/2021-3, 303973/2023-4, 408475/2023-4, 301820/2025-2).

Appendix A. Supplementary data

Supplementary data to this article can be found online at https://doi.org/10.1016/j.tet.2026.135195.

Data availability

Data will be made available on request.

References

[1] C.M. Marshall, J.G. Federice, C.N. Bell, P.B. Cox, J.T. Njardarson, J. Med. Chem. 67 (2024) 11622–11655.
[2] (a) P.S. Auti, G. George, A.T. Paul, RSC Adv. 10 (2020) 41353–41392; (b) L.S. Franco, P.S.M. Pinheiro, M.L.C. Barbosa, J. Braz. Chem. Soc. 35 (2024) e-20240100; (c) H.A.M. Gomaa, Chem. Biol. Drug Des. 100 (2022) 639–655.
[3] S. Singh, D. Utreja, V. Kumar, Med. Chem. Res. 31 (2022) 1–25.
[4] (a) R. Tamatam, S.H. Kim, D. Shin, Front. Chem. 11 (2023) 1140562; (b) S. Khabnadideh, S. Sadeghian, J. Chem. 2022 (2022) 8424838.
[5] (a) G.S. Rai, J.J. Maru, Chem. Heterocycl. Compd. 56 (2020) 1517–1522; (b) V.R.D. Pereira, G.F. Vargas, T.C. Braga, J.A. dos Santos, G.C. Clososki, J.A. R. Nallar, V.D. Pinho, G.W. Amarante, Eur. J. Org. Chem. 28 (2025) e202500512.
[6] N.J. Castellino, A.P. Montgomery, J.J. Danon, M. Kassiou, Chem. Rev. 123 (2023) 8127–8153.
[7] (a) M.K. Yadav, S. Chowdhury, Org. Biomol. Chem. 23 (2025) 506–545; (b) P. Ye, Y.Y. Xiong, B. Zhang, Tetrahedron Lett. 155 (2025) 155440.
[8] S. Ghara, P. Barik, S. Ghosh, S. Ghosh, A. Mandal, C. Pramanik, M. Ikbal, S. Dhara, S. Samanta, Org. Chem. Front. 12 (2025) 2790–2837.
[9] (a) P. Ghosh, B. Ganguly, S. Das, Org. Biomol. Chem. 18 (2020) 4497–4518; (b) N. Umadevi, G. Kumar, N.C.G. Reddy, B.V.S. Reddy, Curr. Org. Chem. 25 (2021) 601–634.
[10] (a) X. Liu, D. Xie, Q. Yang, Z. Song, Y. Fu, Y. Peng, Org. Biomol. Chem. 22 (2024) 7725–7735; (b) R.D. Mandal, M. Saha, D. Das, A.R. Das, J. Org. Chem. 88 (2023) 6071–6095.
[11] E. Zarenezhad, S. Behrouz, M. Farjam, M.N.S. Rad, Russ. J. Bioorg. Chem. 47 (2021) 609–621.
[12] C. Obradors, B. Mitschke, M.H. Aukland, M. Leutzsch, O. Grossmann, S. Brunen, S. A. Schwengers, B. List, Angew. Chem. Int. Ed. 61 (2022) e202114619.
[13] (a) X. Luo, Q. Feng, P. Wang, Synthesis 54 (2022) 2696–2706; (b) R.S.J. Proctor, R.J. Phipps, Angew. Chem. Int. Ed. 58 (2019) 13666–13699; (c) Z. Liu, L. Peng, H. Huang, Chem. Commun. 61 (2025) 14490.
[14] A. Guitiérrez-Bonet, C. Remeur, J.K. Matsui, G. Molander, J. Am. Chem. Soc. 139 (2017) 12251.
[15] X. Cheng, F. Ye, X. Luo, X. Liu, J. Zhao, S. Wang, Q. Zhou, G. Chen, P. Wang, J. Am. Chem. Soc. 45 (2019) 18230–18237.
[16] S. Wang, Q.Q. Zhuo, X. Zhang, P. Wang, Angew. Chem. Int. Ed. 61 (2022) e202111388.
[17] (a) J.A. Dantas, R. Echemendía, M.S. Santos, M.W. Paixão, M.A.B. Ferreira, A. G. Corrêa, J. Org. Chem. 85 (2020) 11663–11678; (b) M.A.P. Januário, D.P. de Souza, J. Zukerman-Schpector, A.G. Corrêa, ChemistryOpen 12 (2023) e202300070.
[18] X. Chen, X. Luo, K. Wang, F. Liang, P. Wang, Synlett 32 (2021) 733–737.
[19] T. Shang, L. Lu, Z. Cao, Y. Liu, W. He, B. Yu, Chem. Commun. 55 (2019) 5408–5419.
[20] (a) X. Chen, Z. Quan, X. Wang, Appl. Organomet. Chem. 29 (2015) 296–300; (b) T. Xing, Z. Zhang, Y. Da, Z. Quan, X. Wang, Asian J. Org. Chem. 4 (2015) 538–544.
[21] W. Liu, Y. Feng, S. Yu, Z. Fan, X. Li, J. Li, H. Yin, Int. J. Mol. Sci. 22 (2021) 12824.
[22] V. Šlachtová, S. Bellová, A. La-Venia, J. Galeta, M. Dračínský, K. Chalupský, A. Dvořáková, H. Mertlíková-Kaiserová, P. Rukovanský, R. Dzijak, M. Vrabel, Angew. Chem. Int. Ed. 62 (2023) e202306828.
[23] J.J.A. Garwood, A.D. Chen, D.A. Nagib, J. Am. Chem. Soc. 146 (2024) 28034–28059.
[24] C.G.S. Lima, T. de M. Lima, M. Duarte, I.D. Jurberg, M.W. Paixão, ACS Catal. 6 (2016) 1389–1407.
[25] (a) Y. Yuan, S. Majumder, M. Yang, S. Guo, Tetrahedron Lett. 61 (2020) 151506; (b) A.K. Wortman, C.R.J. Stephenson, Chem 9 (2023) 2390–2415.
[26] M.C. Casanova, M. Fil, Y. Zhao, N. Azas, S. Redon, P. Vanelle, J. Broggi, Synlett 34 (2023) 1685–1688.
[27] L. Yang, H. Luo, Y. Sun, Z. Shi, K. Ni, F. Li, D. Chen, Synthesis 49 (2017) 2535–2543.
[28] P.G. Dalai, N. Panda, Adv. Synth. Catal. 364 (2022) 3736–3742.
[29] B. Liu, Q. Wang, B. Cheng, T. Wang, H. Liao, H.W. Lin, Green Chem. 26 (2024) 4742–4748.
[30] Y. Gao, Z. Wu, L. Yu, Y. Wang, Y. Pan, Angew. Chem. Int. Ed. 59 (2020) 10859–10863.
[31] L.I. Panferova, M.O. Zubkov, V.A. Kokorekin, V.V. Levin, Angew. Chem. Int. Ed. 133 (2021) 2885–2890.
[32] I. Sokolovs, E. Suna, Org. Lett. 25 (2023) 2047–2052.